PHYSICAL REVIEW A **73**, 011603(R) (2006)

Measurement of the electric polarizability of lithium by atom interferometry

A. Miffre, M. Jacquey, M. Büchner, G. Trénec, and J. Vigué*
Laboratoire Collisions Agrégats Réactivité IRSAMC, Université Paul Sabatier and CNRS UMR 5589 118, Route de Narbonne 31062 Toulouse Cedex, France
(Received 14 June 2005; published 30 January 2006)

We have built an atom interferometer and, by applying an electric field on one of the two interfering beams, we have measured the static electric polarizability of lithium $\alpha=(24.33\pm0.16)\times10^{-30}$ m^3 with a 0.66% uncertainty. Our experiment is similar to an experiment done on sodium in 1995 by Pritchard and co-workers, with several improvements: the electric field can be calculated analytically and the interference signals have a large intensity and a high visibility, resulting in accurate phase measurements. This experiment illustrates the extreme sensitivity of atom interferometry: when the atom enters the electric field, its velocity increases and the fractional change, equal to 4×10^{-9} for our largest field, is measured with a 10^{-3} accuracy.

DOI: 10.1103/PhysRevA.73.011603 PACS number(s): 03.75.Dg, 32.10.Dk, 32.60.+i, 39.20.+q

An atom interferometer is the ideal tool to measure any weak perturbation of the atom propagation due to electromagnetic or inertial fields. The application of a static electric field gives access to the electric polarizability α and this quantity cannot be measured by spectroscopy which is sensitive only to polarizability differences. Atom electric polarizabilities are related to many important physical quantities as pointed out in the book by Bonin and Kresin [1].

Several experiments with atom interferometers have exhibited a sensitivity to the electric field [2,3] without aiming at a polarizability measurement and interferometers using an inelastic diffraction process have been used to measure the polarizability difference between two states [4,5]. An accurate measurement of the atom polarizability α requires that a well-defined electric field is applied on only one interfering beam and, up-to-now such an experiment has been made only by Pritchard *et al.* [6,7] by inserting a thin electrode, a septum, between the two atomic paths. We have made a similar experiment with our lithium atom interferometer, represented in Fig. 1 and we are going to describe its results. With respect to the experiment of Pritchard *et al.*, we have made several improvements: the electric field of our capacitor is analytically calculable; our phase sensitivity is larger; finally our interferometer is species selective, thanks to laser diffraction. Our accuracy is limited by the knowledge of the mean atom velocity.

When an electric field E is applied, the ground-state energy decreases by the polarizability term $U=-2\pi\epsilon_0\alpha E^2$. Therefore, when an atom enters the electric field, its kinetic energy increases and its wave vector k becomes $k+\Delta k$, with $\Delta k=2\pi\epsilon_0\alpha E^2 m/(\hbar k)$. The resulting phase shift ϕ of the atomic wave is given by

$$\phi=\frac{2\pi\epsilon_0\alpha}{\hbar v}\int E^2(z)dz. \tag{1}$$

$v=\hbar k/m$ is the atom velocity and the spatial dependence of the electric field along the atomic path is taken into account.

To know precisely the electric field along the atomic path, guard electrodes are needed, as discussed in Ref. [6]. In our capacitor (see Fig. 2 which defines the notations), guard electrodes are in the plane of the high voltage electrode so that the field can be expressed analytically from the potential distribution $V(z,x=h)$ in the plane of the high-voltage electrode. This calculation will be published elsewhere [8]. The integral of E^2 along the septum surface is equal to

$$\int E(z,0)^2dz=[V_0/h]^2L_{eff}. \tag{2}$$

V_0/h is the electric field of an infinitely long capacitor and the capacitor effective length L_{eff} is given by

$$L_{eff}\approx 2a-(2h/\pi), \tag{3}$$

neglecting corrections of the order of $\exp(-2\pi a/h)$. The atoms sample the electric field at a small distance x from the septum and the corresponding correction to the effective length, which is proportional to x^2, is smaller than $10^{-4}L_{eff}$ in our experiment.

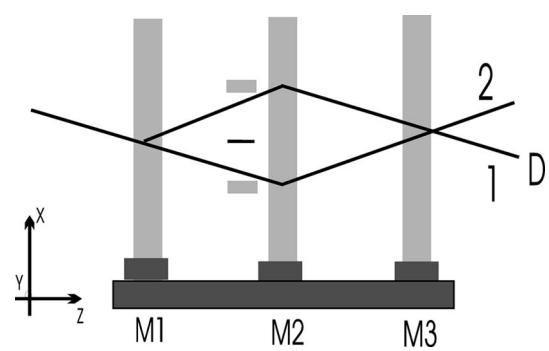

FIG. 1. Schematic drawing of our Mach-Zehnder atom interferometer: a collimated atomic beam, coming from the left, is diffracted by three laser standing waves and the output beam 1 selected by a slit is detected by a hot-wire detector D. The capacitor with a septum is placed just before the second laser standing wave. The x, y, and z axis are defined.

*Electronic address: jacques.vigue@irsamc.ups-tlse.fr

 ©2006 The American Physical Society

The capacitor external electrodes are made of thick glass plates covered by an aluminum layer. The guard electrodes are insulated from the high voltage electrode by 100-μm-wide gaps which have been made by laser evaporation and, under vacuum, we can operate the capacitor up to $V=450$ V. The glass spacers are glued on the external electrodes and the septum, made of a 6-μm-thick Mylar foil aluminized on both faces, is stretched and glued on the electrode-spacer assemblies. In our calculation, we assume that the potential on the high-voltage electrode is known everywhere but the potential inside the 100-μm-wide dielectric gaps is unknown if these gaps get charged. This is unlikely because of the finite but nonzero conductivity of the glass plates [8] but a superiority of our design is that these gaps are very narrow, thus minimizing the uncertainty on the capacitor effective length. Another defect is that the spacer thicknesses are not perfectly constant. We use Eq. (2) by replacing h by its mean value $\langle h\rangle$, thus making a relative error of the order of $\langle(h-\langle h\rangle)^2\rangle/\langle h\rangle^2$ which is fully negligible.

In our three-grating Mach-Zehnder atom interferometer [9,10], we use a supersonic beam of lithium seeded in argon and Bragg diffraction on laser standing waves at $\lambda=671$ nm. By choosing a laser detuned by about 3 GHz on the blue side of the $^2S_{1/2}$-$^2P_{3/2}$ transition of the ^{7}Li isotope, the signal is almost purely due to this isotope (natural abundance 92.4%) and not to the other isotope ^{6}Li. Any other species present in the beam, lithium dimers or heavier alkali atoms, is not diffracted and does not contribute to the signal. In three-grating interferometers, the phase of the interference fringes depends on the x position of the gratings depending themselves on the position x_i of the mirrors M_i forming the three laser standing waves and this phase is given by $\psi=2pk_L(x_1+x_3-2x_2)$, where k_L is the laser wave vector and p is the diffraction order. By scanning the position x_3 of mirror M_3, we have observed interference fringes with an excellent visibility $\mathcal{V}$, up to 84.5%.

The capacitor is placed just before the second laser standing wave, with the septum between the two atomic beams (see Fig. 1). In the present work, we have used only the diffraction order $p=1$ so that the center of the two beams are separated by about 90 μm in the capacitor. When the septum is inserted between the two atomic paths, the atom propagation is almost not affected and we observe interference fringes with a visibility $\mathcal{V}=84\%$ and a negligible reduction of the atomic flux. To optimize the phase sensitivity, we have opened the collimation slit S_1 and the detection slit S_D (see reference [10]) with widths $e_1=18$ μm and $e_D=50$ μm, thus increasing the mean flux up to 10^5 counts/s and slightly reducing the fringe visibility down to $\mathcal{V}_0=62\%$ (see Fig. 3). We have made a series of recordings, labeled by an index i from 1 to 44, with $V_0=0$ when i is odd and with $V_0\neq 0$ when i is even with $V_0\approx 10i$ V. For each recording, we apply a linear ramp on the piezo-drive of mirror M_3 in order to observe interference fringes and 471 data points are recorded with a counting time per channel equal to 0.36 s. Figure 3 presents a pair of consecutive recordings. The high voltage power supply has a stability close to 10^{-4} and the applied voltage is measured by a HP 34401A voltmeter with a relative accuracy better than 10^{-5}.

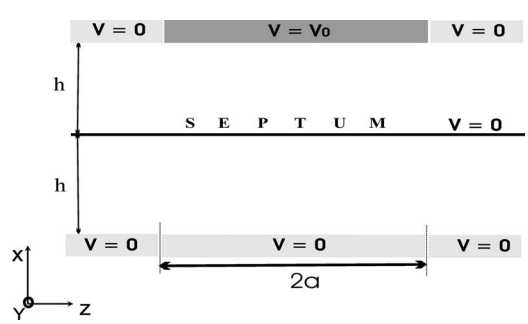

FIG. 2. Schematic drawing of the capacitor. The septum is parallel to the z axis and the electrodes are located at $x=\pm h\approx 2$ mm. The high voltage electrodes at the potential V_0 extends from $z=-a$ to $z=+a$, while the guard electrodes extend outside with $|z|>a$, with $a\approx 25$ mm. The septum and the guard electrodes are at $V=0$.

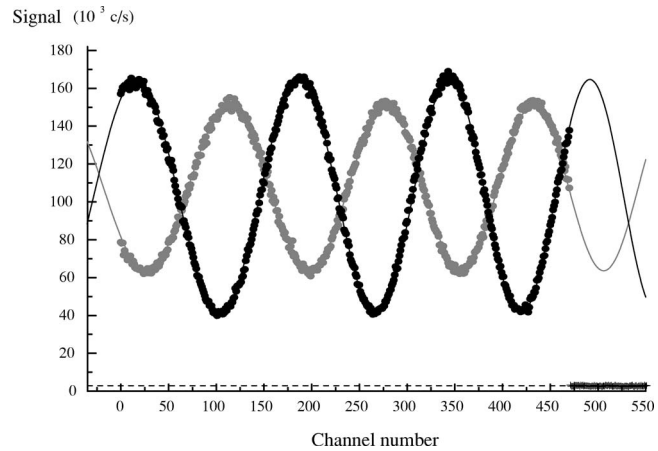

FIG. 3. Experimental signals and their fits (full curves) corresponding to $V=0$ (black dots) and $V_0\approx 260$ V (gray dots): the phase shift is close to 3π with a reduced visibility.

The data points $I_i(n)$ have been fitted by a function $I_i(n)=I_{0i}[1+\mathcal{V}_i\cos\psi_i(n)]$, with $\psi_i(n)=a_i+b_in+c_in^2$ where n labels the channel number, a_i represents the initial phase of the pattern, b_i an ideal linear ramp and c_i the nonlinearity of the piezodrive. For the $V=0$ recordings, a_i, b_i, and c_i have been adjusted as well as the mean intensity I_{0i}, and the visibility $\mathcal{V}_i$, while, for the $V\neq 0$ recording, we have fitted only a_i, I_{0i}, and $\mathcal{V}_i$, while fixing b_i and c_i to their values b_{i-1} and c_{i-1} from the previous $V=0$ recording. Our best phase measurements are given by the mean phase $\bar{\psi}_i$ obtained by averaging $\psi_i(n)$ over the 471 channels. The 1σ error bars of these mean phases are of the order of 2–3 mrad, increasing with the applied voltage up to 23 mrad because of the reduced visibility.

The $\bar{\psi}_i$ values of the $V_0=0$ recordings present a drift, equal to 7.5 ± 0.2 mrad/minute, which is due to the differential thermal expansion of the rail supporting the three mirrors: its temperature was steadily drifting at 1.17×10^{-3} K/min during the experiment. In addition to this drift, there is also some scatter with an rms value equal to 33 mrad and a quasiperiodic structure as a function of time. We have no explanation for this scatter which gives the dominant contribution to the uncertainty of our phase shift measurement.

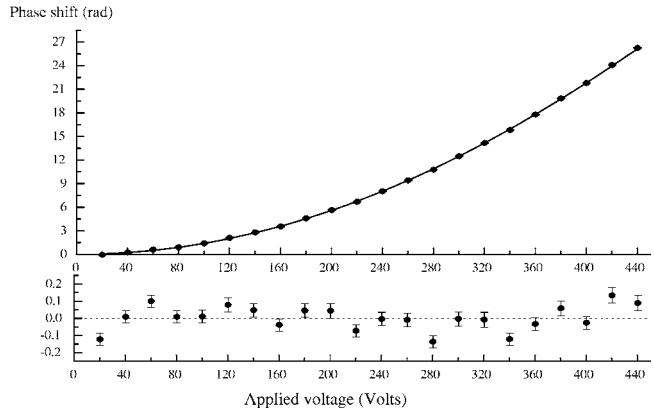

FIG. 4. Phase shift $\langle\phi(V_0)\rangle$ as a function of the applied voltage V_0: the best fit using Eqs. (4) and (5) is represented by the full curve and the residuals are plotted in the lower graph.

The phase shift $\langle\phi(V_0)\rangle$ due to the polarizability effect (the average $\langle\ \rangle$ recalls that our experiment makes an average over the velocity distribution, as discussed below) is taken equal to $\langle\phi(V_0)\rangle=\bar{\psi}_i-(\bar{\psi}_{i-1}+\bar{\psi}_{i+1})/2$ where the recording i corresponds to the applied voltage V_0: the average of the mean phase of the two $V_0=0$ recordings done just before and after is our best estimator of the mean phase of the interference signal in zero field and we evaluate the error bar on $\langle\phi(V_0)\rangle$ by combining quadratically the error bar on $\bar{\psi}_i$ with the 33 mrad error bar estimated above for the zero field phase. In Figs. 4 and 5, we have plotted the phase shift $\langle\phi(V_0)\rangle$ and the fringe visibility $\langle\mathcal{V}\rangle$ as a function of the applied voltage V_0.

The phase shift, proportional to v^{-1}, must be averaged over the atom velocity distribution $P(v)$:

$$P(v)=\frac{S}{u\sqrt{\pi}}\exp\{-[(v-u)S\|/u]^2 \tag{4}$$

with the most probable velocity u and $S_\|$ is the parallel speed ratio. We have omitted the traditional v^3 prefactor [11] which

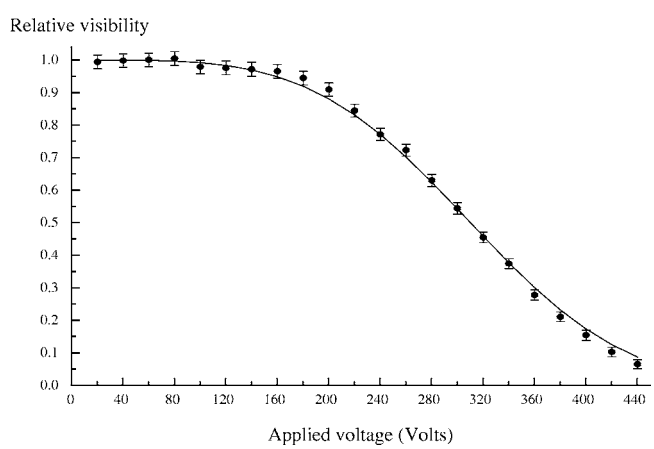

FIG. 5. Relative fringe visibility $\langle\mathcal{V}\rangle/\mathcal{V}_0$ (with $\mathcal{V}_0=62\%$) as a function of the applied voltage V_0 and the best fit using Eqs. (4) and (5) (full curve).

has minor effects when $S_\|$ is large. The interference signals I can be written:

$$\begin{aligned} I &= I_0\int dv P(v)\left[1+\mathcal{V}_0\cos\left(\psi+\phi_m\frac{u}{v}\right)\right] \\ &= I_0[1+\langle\mathcal{V}\rangle\cos(\psi+\langle\phi\rangle)] \end{aligned} \tag{5}$$

where ϕ_m is the value of the phase ϕ for the velocity $v=u$. It is necessary to calculate this integral (5) numerically and we have made a single fit for the phase and visibility results, with two adjustable parameters: $\phi_m(V_0)/V_0^2$ and $S_\|$. As shown in Figs. 4 and 5, the agreement is very good, in particular for the phase shifts, and we deduce the value of $\phi_m(V_0)/V_0^2$,

$$\phi_m(V_0)/V_0^2=(1.3870\pm0.0010)\times10^{-4}\text{rad/V}^2, \tag{6}$$

with a relative uncertainty equal to only 0.07%. The parallel speed ratio $S_\|=8.00\pm0.06$ is slightly larger than expected, because Bragg diffraction is velocity selective.

We have measured the capacitor plate spacing h with a Mitutoyo Litematic machine with 1 μm accuracy and we get $\langle h\rangle=2.056\pm0.003$ mm. We also get $2a=50.00\pm0.10$ mm. We have measured the mean velocity u using Doppler effect, by recording atom deflection due to photon recoil with a laser beam almost counterpropagating with the atoms. The uncertainty on the cosine of the angle is negligible (0.12%) and we get $u=1066.4\pm8.0$ m/s. We have also recorded the diffraction probability as a function of the Bragg angle, by tilting the mirror forming a standing wave. Using an independent calibration of the mirror rotation as a function of the applied voltage on the piezodrive, we get a measurement of the Bragg angle $\theta_B=h/(mu\lambda_L)=79.62\pm0.63$ μrad corresponding to $u=1065.0\pm8.4$ m/s. These two measurements of u are perfectly coherent and we take their weighted average $u=1065.7\pm5.8$ m/s. The theory of supersonic expansion can be used to check this result. The velocity of a pure argon beam given by $u=\sqrt{5k_BT_0/m}$ (where $T_0=1073\pm11$ K is the nozzle temperature and m the argon atomic mass) must be corrected, the dominant correction being due to the velocity slip effect, estimated to be 2.42% [12], and we get $u=1073.0\pm5.6$ m/s, in good agreement with our measurements.

We thus get the electric polarizability of ^{7}Li $\alpha=(24.33\pm0.16)\times10^{-30}$ m$^3=164.2\pm1.1$ atomic units (a.u.), in excellent agreement with previous measurements, $\alpha=(22.\pm2.)\times10^{-30}$ m^3, by Chamberlain and Zorn [13] in 1963, and $\alpha=(24.3\pm0.5)\times10^{-30}$ m^3, by Bederson and co-workers [14] in 1974. Many calculations of α are available [15]. The converged Hartree-Fock value [16] is $\alpha=169.946$ a.u. and the most accurate calculations with electron correlation were obtained in 1994 by Kassimi and Thakkar [16] with a Möller-Plesset calculation, $\alpha=164.2\pm0.1$ a.u., and in 1996 by Drake and co-workers [17] with an Hylleraas calculation, $\alpha=164.111\pm0.002$ a.u. Our result, which differs substantially from the Hartree-Fock value, agrees with these very accurate calculations, which still neglect relativistic corrections (about −0.06 a.u. [18]) and finite nuclear mass correction of comparable magnitude.

With respect to the sodium polarizability measurement of Ref. [6], we have made several improvements:

Our capacitor design provides an analytical calculation of the E^2 integral, so that we can understand the influence of defects and minimize the uncertainty on this integral. An improved construction should reduce the uncertainty on this integral near 0.1%.

Laser diffraction makes our interferometer species selective, which is a very favorable circumstance. In Ref. [19], Roberts has reanalyzed the measurement of sodium electric polarizability of Ref. [6] and he estimates that the contribution of sodium dimers to the interference signals might have introduced a 2% error in the polarizability value.

Thanks to a large signal and an excellent fringe visibility, the phase sensitivity of our interferometer is considerably larger than previously achieved. The accuracy of our phase measurements, presently limited by small phase jumps between consecutive recordings, is illustrated by the quality of the fit of Fig. 4 and by the 0.07% uncertainty of $\phi_m(V_0)/V_0^2$. The relative uncertainty on the electric polarizability α, dominated by the uncertainty on the mean atom velocity u, is equal to 0.66%. Recently, Amini and Gould [20] using an atomic fountain have measured the polarizability of cesium atom with an even smaller relative uncertainty, equal to 0.14%.

Roberts *et al.* [7] have devised a very clever technique to correct for the velocity dependence of the phase shift ϕ, so that they can observe fringes with a good visibility up to very large ϕ values. In the present work, a very accurate measurement has been done in the presence of an important velocity dispersion without any compensation of the phase dispersion, by including the velocity distribution in the analysis. A velocity measurement remains necessary and we think that the techniques introduced in reference [7] can be used to make a velocity measurement detected on interference signals.

Finally, we would like to emphasize two striking properties of atom interferometry. The phase measurement consists in measuring the increase Δv of the atom velocity v when entering the field,

$$\frac{\Delta v}{v} = \frac{\lambda_{dB}}{L_{eff}} \frac{\phi}{2\pi}. \tag{7}$$

$\Delta v/v$ is extremely small, reaching only $\Delta v/v \approx 4\times 10^{-9}$ for our largest field. Our ultimate sensitivity, close to a 3 mrad phase shift, corresponds to $\Delta v/v \approx 6\times 10^{-13}$.

In the capacitor, the atom wave function samples two regions of space separated by ~ 100 μm with a macroscopic object lying inbetween and this situation extends over 10^{-4} s, *without* any loss of coherence. This consequence of quantum mechanics remains surprising.

We thank J. C. Lehmann and J. F. Arribart, J. F. Bobo and M. Nardone, F. Nez and F. Biraben, and the staff of the AIME for their help. We thank CNRS SPM and Région Midi Pyrénées for financial support.

[1] K. D. Bonin and V. V. Kresin, *Electric-Dipole Polarizabilities of Atoms, Molecules and Clusters* (World Scientific, Singapore, 1997).
[2] F. Shimizu, K. Shimizu, and H. Takuma, Jpn. J. Appl. Phys., Part 1 **31**, L436 (1992).
[3] S. Nowak, N. Stuhler, T. Pfau, and J. Mlynek, Phys. Rev. Lett. **81**, 5792 (1998); Appl. Phys. B **69**, 269 (1999).
[4] V. Rieger *et al.*, Opt. Commun. **99**, 172 (1993).
[5] A. Morinaga *et al.*, Phys. Rev. A **54**, R21 (1996).
[6] C. R. Ekstrom *et al.*, Phys. Rev. A **51**, 3883 (1995).
[7] T. D. Roberts *et al.*, Phys. Rev. Lett. **92**, 060405 (2004).
[8] A. Miffre *et al.*, Eur. Phys. J. D (to be published).
[9] R. Delhuille *et al.*, Appl. Phys. B **74**, 489 (2002).
[10] A. Miffre *et al.*, Eur. Phys. J. D **33**, 99 (2005).
[11] H. Haberland, U. Buck, and M. Tolle, Rev. Sci. Instrum. **56**, 1712 (1985).
[12] P. A. Skovorodko, *24th Rarefied Gas Dynamics*, AIP Conf. Proc. No. 762 (AIP, New York, 2005) P. 857; (private communication).
[13] G. E. Chamberlain and J. C. Zorn, Phys. Rev. **129**, 677 (1963).
[14] R. W. Molof *et al.*, Phys. Rev. A **10**, 1131 (1974).
[15] F. W. King, J. Mol. Struct.: THEOCHEM **400**, 7 (1997).
[16] N. E. Kassimi and A. J. Thakkar, Phys. Rev. A **50**, 2948 (1994).
[17] Z. C. Yan *et al.*, Phys. Rev. A **54**, 2824 (1996).
[18] I. S. Lim *et al.*, Phys. Rev. A **60** 2822 (1999).
[19] T. D. Roberts, Ph. D. thesis, MIT, 2002 (unpublished).
[20] J. M. Amini and H. Gould, Phys. Rev. Lett. **91**, 153001 (2003).